Assessment of the CINEMA Code Prediction of the QUENCH-06 Experiment

Hyoung Tae Kim [a*] and Sang Ho Kim [a]
Intelligent Accident Mitigation Research Division, KAERI, Daeduk-daero 989-111, Daejeon, Korea
[*]*Corresponding author: kht@kaeri.re.kr*

1. Introduction

The QUENCH-06 test [1] exercise was performed by the IAEA CRP (Coordinate Research Project) participants in sophistication and quality of severe accident analyses with various codes that generated new knowledge relevant to evaluation of uncertainties and sensitivity analysis of severe accident simulation and modelling [2]. In this study the CINEMA (Code for INtegrated severe accidEnt Management and Analysis) [3] code is used to simulate the QUENCH-06 test and its simulation results are compared with those by MELCOR and SPACE codes, as well as test data.

The QUENCH-06 experiment was conducted at the Karlsruhe Institute of Technology on December 2000 (KIT, Germany). The main objective of QUENCH-06 is to investigate fuel rod bundle behavior up to and during reflood/quench conditions without severe fuel rod damage prior to reflood initiation [4].

The user input parameters of the CINEMA code (ver. 385) for prediction of the QUENCH-06 should be optimized for the best estimation of the code capability. Therefore, other severe accident analysis code, MELCOR is referenced to determine the input parameters of the radiation heat transfer, which is the most effective heat transfer for prediction of the temperature measurements. The MELCOR ver1.8.6 [5] and SPACE codes with heat structure model are also utilized to investigate the sensitivity of the input parameters.

2. Overview of the QUENCH-06 Experiment

2.1 Description of the test facility

The QUENCH facility simulates the fuel rods with the out of pile bundle. This bundle consists of a 5 × 5 structure made up of 21 fuel simulator rods and 4 corner rods fixed by five grid spacers (Fig. 1). This bundle includes 20 heated rods, one unheated central rod that can be used for measurement devices or as a control rod, and four corner rods. The overall length of the rods is approximately 2.5 m, and the heating length is about 1 m. The cladding is a zirconium alloy Zircaloy-4 with an outer diameter of 10.75 mm and a wall thickness of 0.725 mm. A tungsten heater at the center of each heated rod has an outside diameter of 6 mm. ZrO_2 pellets surround the tungsten heaters of the heated rods, whereas the unheated central rod is totally filled with ZrO_2 pellets without the heater.

The bundle is surrounded by a shroud of three layers. The first one is made of Zircaloy at the inner side (outer diameter: ～85 mm), followed by a central ZrO_2 fiber insulation layer and an annular stainless steel cooling jacket.at the outer side, to provide the encasement of the bundle.

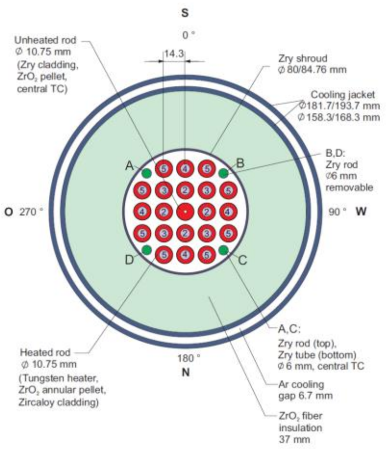

(a) cross section, top view

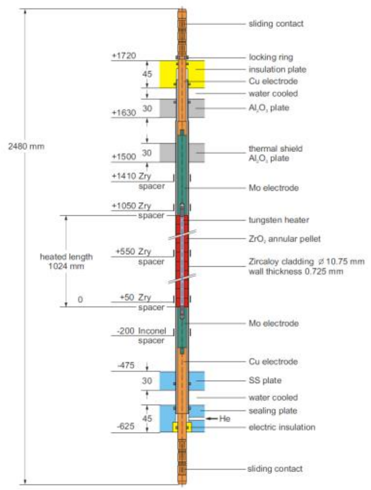

(b) axial view (heated rod)

Fig. 1. Fuel rod simulator bundle including rod type indications of the QUENCH test facility [4].

A simplified flow diagram of the QUENCH test facility is shown in Fig. 2. The pressure in the test section is usually ~0.2MPa. The superheated steam and argon as the carrier gas for the hydrogen detection systems enter the test bundle at the bottom end. Argon, steam, and H_2 produced in the zirconium–steam reaction flow upward inside the bundle. Once reached the top, the mixture flows through a water cooled off-gas pipe to the condenser, where the not condensed steam is separated from the non-condensable gases (usually argon and H_2). The quenching phase is initiated by turning off the superheated steam of 3 g/s whereas the argon flow rate remains unchanged but the gas inlet position is switched to the upper plenum of the test section. At the same time quenching water is injected at the bottom of the test bundle through a separate line.

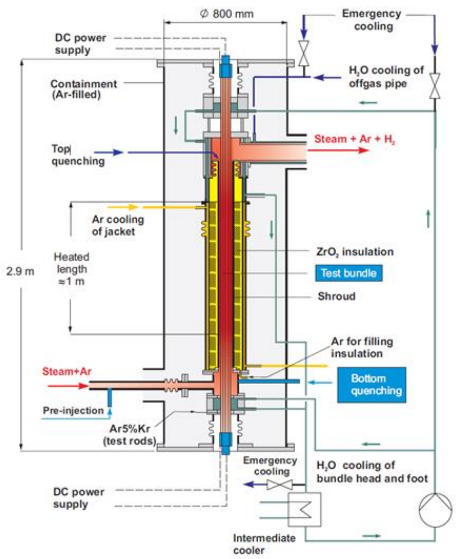

Fig. 2. Flow diagram of the QUENCH test facility [4].

2.2 Test procedures

The sequence of events and phases of QUENCH-06 [2] is shown in Table 1.

Table 1: Sequence of events and phases of the QUENCH-06 experiment

Time(s)	Event	Phase
0	Start of data recording	
30	Heat up to about 1500 K	Heat-up
1965	Pre-oxidation at about 1500 K	Pre-oxidation
6010	Start of the power transient	
6620	Withdrawal of the corner rod B	Transient
7179	Shut down of the steam supply, fast water injection, switch of the argon supply	
7181	Steam mass flow rate at zero	
7205	Start of the electrical power reduction to 4 kW	Reflooding
7221	Decay heat level reached	
7431	Shut down of the quench water injection, electrical power shut off	
11,420	End of data acquisition	

The first operational phase is a heat-up phase, when the bundle was brought to an intermediate temperature level (～1500 K). The second is a pre-oxidation phase, when the temperature was kept constant up to the time at which the maximum oxide layer reached the experiment designed value. The third is a transient phase, when the temperature increased up to the experiment designed value for the onset of quenching phase. The last of the operational phases is a reflood phase, when the steam supply was stopped and water was added, simulating the reflood.

The bundle is heated (see Fig. 3) by a series of stepwise increase of the electrical power up to 4 kW from room temperature to 873 K in an atmosphere of flowing Argon (3 g/s) and steam (3 g/s). Figure 4 shows the flow behavior of the working fluids in the test section.

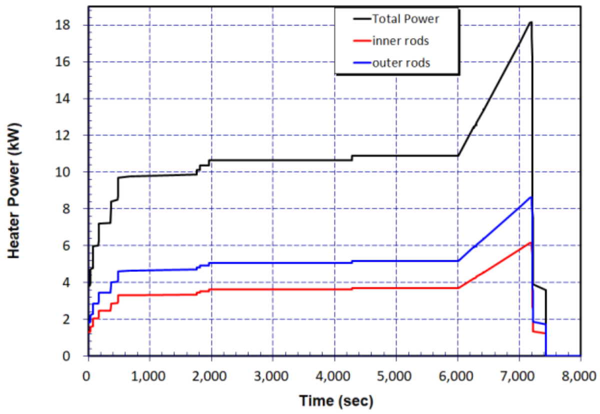

Fig. 3. Power history of the QUENCH-06 test.

At the end of such stabilization period, the pre-oxidation phase begins: the power is increased up to 10.5 kW and the maximum axial temperature is maintained constant at 1473 K for 4046 s. The transient phase beings at 6010 s and it is triggered by ramping the electrical power of the bundle at 0.3 W/s/rod between 1450 K and 1750 K, based on the thermocouple signal at 950 mm elevation. During the transient phase and before any temperature excursion the corner rod B (Fig. 1) is withdrawn at 6620 s to evaluate the oxidation at that time.

The quench phase begins at 7179s when the temperature of the central rod has reached ~1873 K and the temperature of at least three rods exceeds 1973 K.

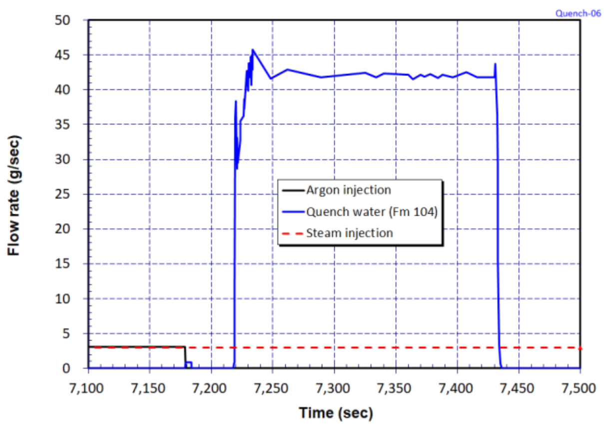

Fig. 4. Argon, steam, and quench water flow rates.

About 20 s after the reflood injection, the electrical power is reduced to about 4 kW within 15 s, to simulate the decay heat levels. The flooding of the bundle is terminated when the shroud temperature at 1150 mm height indicates a local wetting. The cooling of the test section to about 400 K is completed at about 250 s after the beginning of the flooding. Few seconds later, the quench water injection and the electrical power are shut off, the experiment being terminated.

3. Code Modeling

3.1 CINEMA Code (ver. 385)

The reference input model of QUENCH-06 experiment was obtained from reference [8]. The nodalization of the test section is shown in Fig. 5.

The CINEMA code utilizes the SPACE code module for general thermal-hydraulic calculations and compass module for severe accident analysis. For the thermal-hydraulic data transfer between SPACE and compass module, Two channels of the SAM nodes are used for region of the inner rods and outer rods, respectively.

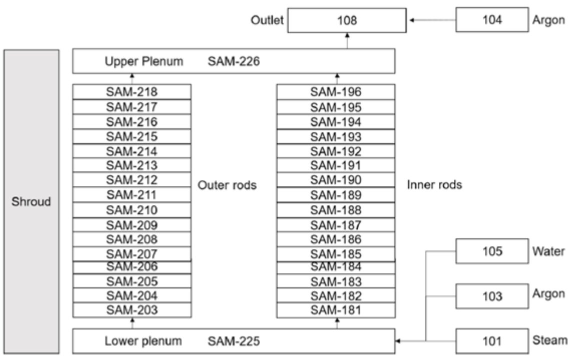

Fig. 5. CINEMA nodalization for QUENCH-06 [8].

3.2 SPACE code and MELCOR Codes with Heat Structure Model

For code comparisons for simulation results, the detailed heat structure models are applied to the SPACE code and MELCOR code. Figure 6 shows the nodalization of code inputs with heat structure models.

○ SPACE input
- BC for inlet and outlet by TFBC
- Thermal-hydraulic cells and junctions
- Heat structures for heat transfer process of convection, conduction, and radiation

○MELCOR with heat structure model input
- CV and FL for inlet and outlet BC, flow channels
- Only using heat structure for heater rods and surrounding shroud structures

○MELCOR with heat structure model input
- COR package used for heater rods and surrounding shroud structures

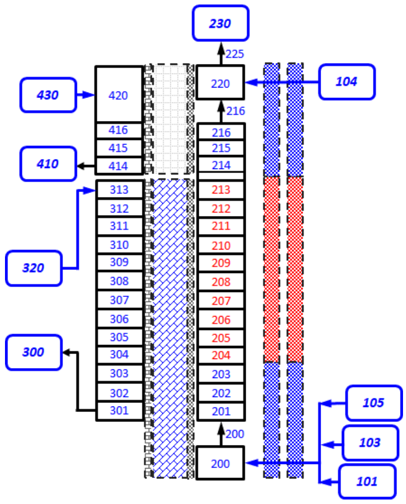

Fig. 6. MELCOR and SPACE nodalization for QUENCH-06 test.

3.3 Main Sensitive Input Parameters

Indirect heating of the heater rods using tungsten and molybdenum wires in the electrode zones simulates the decay heat in the QUENCH experiments. The DC voltage measured in the facility includes the voltage drop at the sliding contacts at both ends of the rods, at wires which lead form the sliding contacts to the power supply, and at screws that fix the wires at their ends [6]. This has to be taken into account correctly model the input of electric power into the bundle.

Therefore, it is concluded that the electric power data should be reduced to predict the temperature behavior of the heater rods and surrounding shroud structure from the sensitivity study of the SPACE and MELCOR calculations. Figure 7 shows the reduced power input used for code calculations, which is compared with the electric power supply data.

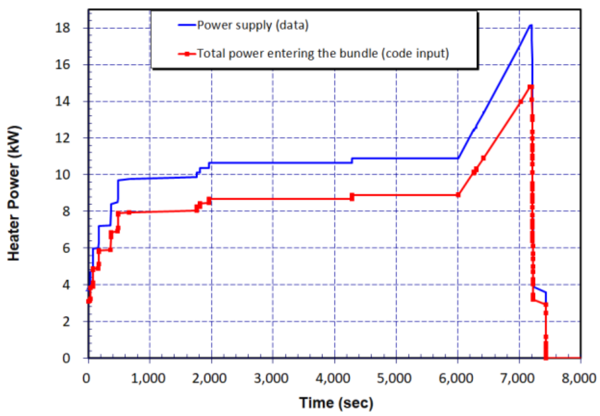

Fig. 7. Comparison of the heater power data with the reduced

power for code input.

Radiation heat transfer from heater rods to surrounding shroud structure walls is also sensitive input parameters for optimal code modeling. For code comparisons of temperature predictions, the view factor and the emissivity values are set to same values in the radiation heat transfer models of the all codes used in this study. Table 2 shows the view factor values used for the wall surfaces participating the radiation heat transfer. The reference emissivity value is set to 0.8 for all code inputs.

Table 2: View factor values used for wall surfaces

From inner rods		From outer rods	
To	View factor	To	View factor
outer rods	0.3915		
corner rods	0.03957	corner rods	0.04606
shroud wall	0.0	shroud wall	0.4379

4. Code Calculation Results

4.1 Code to Code Comparison

The simulation results by the MELCOR (ver.1.86) and SPACE (ver.3.3) with heat structure models are obtained, and compared with those by the CINEMA code.

Wall temperatures of the heater rods in the outer ring region and shroud on the inner wall side are compared with the test data. Figures 8, 9, and 10 are obtained by the SPACE code, MELCOR with heat structure model, and MELCOR with core package model, respectively. The temperature behavior is followed by the power supply transient and the cooling conditions in the heater channel of the test facility. These simulation results are in good agreement with the temperature measurements behavior, except the high temperature peak by steam-zircaloy oxidation.

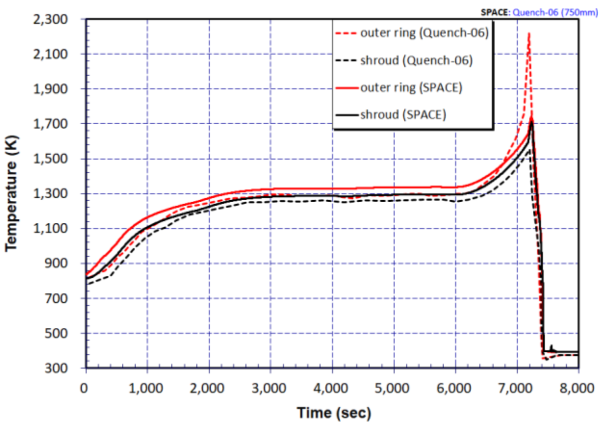

Fig. 8. Temperature predictions by the SPACE code.

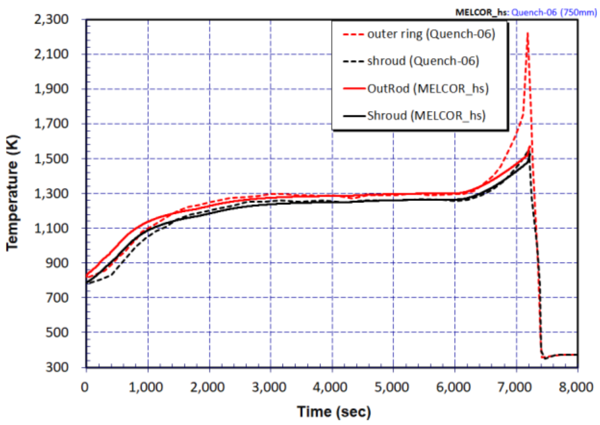

Fig. 9. Temperature predictions by the MELCOR code with heat structure model.

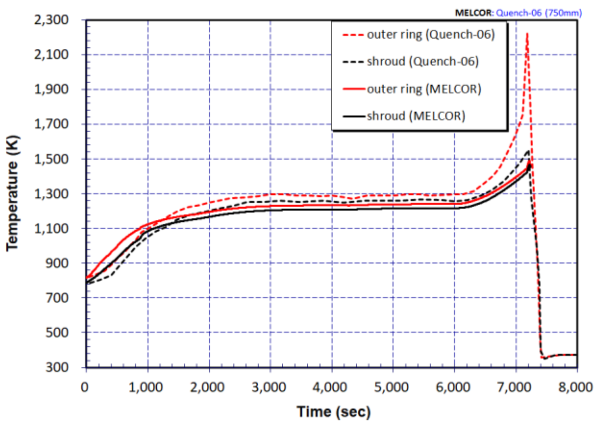

Fig. 10. Temperature predictions by the MELCOR code with core package model.

Figure 11 shows the temperature predictions by the CINEMA code, where the shroud temperature is relatively more under-estimated than those by the SPACE and the MELCOR codes. The CINEMA predictions of the temperature difference between the heater rods (in the outer ring region) and the shroud wall are larger than those by other codes. The radiation heat transfer from the heater rods to shroud wall is the main effective parameter to determine this temperature distance. Therefore, the sensitivity study of the emissivity and view factor between the heater rod and shroud is performed as shown in Figs. 12 and 13, respectively.

The temperature difference between the outer rods and shroud decreases as the emissivity value (Fig. 12) and the view factor (Fig. 13) increase. The enhancement of the radiation heat transfer (increasing of the view factor or emissivity values) leads to decrease the temperature difference among the solid walls participating the radiation heat transfer.

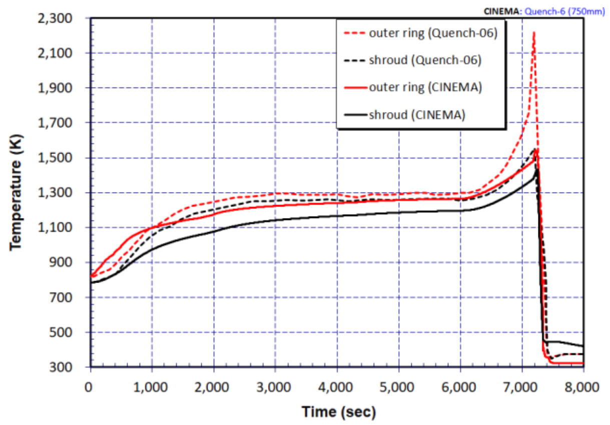

Fig. 11. Temperature predictions by the CINEMA code.

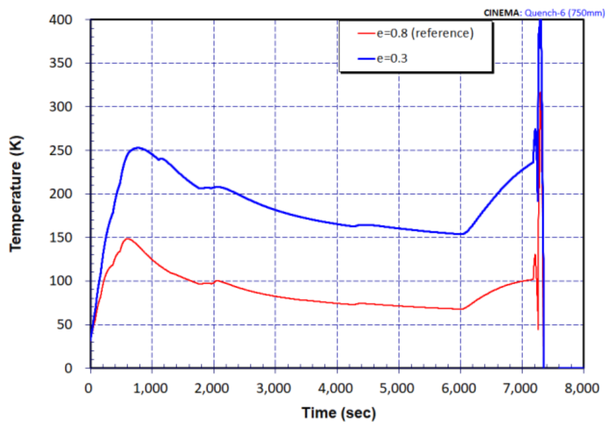

Fig. 12. Sensitivity of emissivity on temperature difference between the outer rods and shroud at elevation of 750mm (CINEMA results).

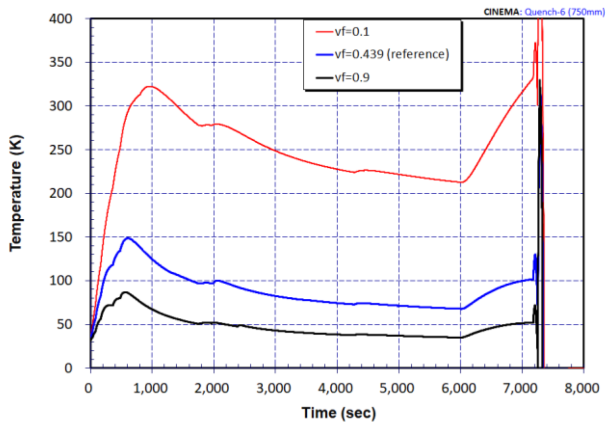

Fig. 13. Sensitivity of view factor on temperature difference between the outer rods and shroud at elevation of 750mm (CINEMA results).

The effect of the view factor on hydrogen generation mass is investigated in Fig. 14. The hydrogen generation mass is dependent on the solid wall temperature participating the steam oxidation. As the view factor between the outer rods and the shroud increases, the temperature of the outer rods in the high temperature region also increase, which results in higher temperature oxidation process and more hydrogen generation mas.

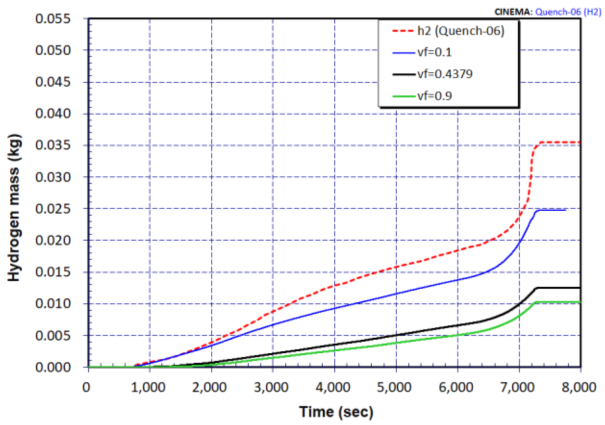

Fig. 14. Sensitivity of view factor on hydrogen generation mass (CINEMA results).

3. Conclusions

The QUENCH-06 test calculation results using the CINEMA, SPACE, and MELCOR codes are presented and compared with each other as well as the test data. To confirm the CINEMA code input modeling is suitable to simulate the QUENCH-06 experiment, the detailed heat structure models are applied to SPACE and MELCOR input models and these code results are used to optimize the main sensitive input parameters of the CINEMA code. For case of the MELCOR code, both input models with heat structure model and with core package model are used to simulate the QUENCH-06 experiment, and these input models are shown to produce the similar results.

The main heat transfer mechanisms found in the QUENCH-06 experiment are gas convection and radiation heat transfer. Steam-zircaloy oxidation is the hydrogen source and temperature excursion at high temperature of solid walls.

The MELCOR and SPACE code with detailed heat structure models are shown to predict well the temperature behavior of the heater rod and shroud and the temperature difference between them. However, the CINEMA code prediction under-estimates the shroud temperature and the temperature difference between outer rods and shroud wall is higher than other code prediction as well as temperature measurement data. From the sensitivity study of emissivity and view factor values of the CINEMA code input model, these parameters are shown to effective to tuning this temperature difference, but it is not sufficient to match the test results. Further study of the CINEMA code input modeling is needed to handle the radiation heat transfer between the hot rods in the core region and surrounding structure of shroud.

All the codes used to simulate the QUENCH-06 experiment in this study could not predict temperature excursion at high temperature peak of solid walls. Therefore, the assessment of the steam oxidation model at high temperature condition for code application is needed for future work.

ACKNOWLEDGMENTS

This work was supported by the Innovative Small Modular Reactor Development Agency grant funded by the Korea Government (MSIT) (No. RS-2023-00259516).

REFERENCES

[1] L. Sepold, et al., Experimental and Computational Results of the QUENCH-06 Test (OECD ISP-45). Report FZKA-6664. Karlsruhe, Germany, 2004.
[2] Advancing the State of the Practice in Uncertainty and Sensitivity Methodologies for Severe Accident Analysis in Water Cooled Reactors in the QUENCH-06 Experiment, IAEA-TECDOC-2045, IAEA Vienna, 2024.
[3] D. H. Kim, J. H. Song, B. C. Lee, J. H. Na, H. T. Kim, Development of an Integrated Severe Accident Analysis Computer Program Packages in Korea, Proceedings of the 8th European Review Meeting on Severe Accident Research (ERMSAR-2017), May 16-18, 2017, Warsaw, Poland.
[4] W. Hering, Ch. Homann, J.-S. Lamy, Comparison Report on the Blind Phase of the OECD International Standard Problem No. 45 Exercise (QUENCH-06), Forschungszentrum Karlsruhe GmbH, Karlsruhe 2002.
[5] R.O. Gauntt et. al., MELCOR Computer Code Manuals, Version 1.8.6, Users Guide and Reference Manual, NUREG/CR-6119, SAND2005-5713, U.S. Nuclear Regulatory Commission, 2005.
[6] Tadas Kaliatka, Algirdas Kaliatka, Virginijus Vileiniškis, and Eugenijus Ušpuras, Modelling of QUENCH-03 and QUENCH-06 Experiments Using RELAP/SCDAPSIM and ASTEC Codes, Science and Technology of Nuclear Installations vol.2014, Article ID 849480
[7] C. Hofmann, W. Hering, A. Miassoedov, L. Sepold, "Detailed Investigation of Thermal-Hydraulics Aspects during the Reflood Phase in QUENCH Experiments", Proc. Of ICONE12, Arlington, Virginia USA, April 25–29 2004.
[8] W. Jeong, D. Son, J. Park Y. H. Jeong, Simulation of high temperature fuel rod bundle behavior during the QUENCH-06 experiment using CINEMA code, Annals of Nuclear Energy vol.182 2023.